A Search for Exclusive Fully Reconstructed W Boson Decays in CDF Run II Data

Dillon Fitzgerald

Wayne State University

Advisor: Professor Robert Harr

(Dated: August 25, 2015)

Abstract

We search for exclusive fully reconstructed $W^+ \to c\bar{s}$ multi-body hadronic decays in CDF Run II data. A fully reconstructed decay of the W boson would provide a new method for measuring the W mass, and could lead to more accurate measurements of production parameters such as rapidity and transverse momentum distributions. Our search includes 87 potential modes of exclusive cascaded $W^+ \to c\bar{s}$ decays, which we aim to reconstruct within the CDF computing framework.

CONTENTS

I. THEORY

A. The Standard Model

The Standard Model of particle physics is a theory that aims to classify all the known subatomic particles, as well as the electomagnetic, strong, and weak interactions. Although the theory is not yet complete, it is the most succesful model to date for describing interactions of subatomic particles. There are still many observed phenomena not described by the Standard Model, some examples being the matter–anti-matter asymmetry observed in the universe, and the currently accepted theory for the gravitational interaction (General Relativity). Subatomic particles are classified as either fermions (quarks and leptons), or bosons (force carriers). There are three generations of fermions, each successive generation becoming heavier and more unstable than the previous. A diagram of the elementary particles of the standard model of particle physics is pictured in Fig 1.

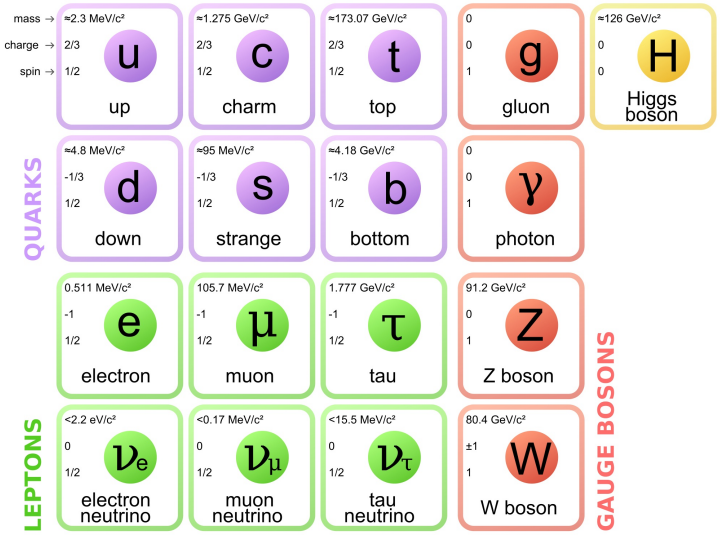

FIG. 1. Elementary Particles of the Standard Model of Particle Physics

Quarks are the only class of subatomic particle that interact via the strong force, and have what is called color charge. Due to a phenomenon in quantum chromodynamics known as color confinement, quarks cannot be isolated because of their color charge and therefore clump together to form colorless groupings called hadrons [1]. The particles detected which we use to reconstruct $W^+ \to c\bar{s}$ decays consist solely of hadrons, as the hadronization process takes place immediately after the W decays into quarks. There are two classes of hadrons; mesons (quark anti-quark pair) and baryons (three quarks), both of which are relevant to our search.

B. W Boson

The W boson was discovered in 1983 at CERN, confirming its prediction in electroweak unification theory proposed in the 1960s. The discovery was made using a $p\bar{p}$ collider [1], where $u\bar{d} \to W^+$ and $\bar{u}d \to W^-$ production was first observed. The W boson is one of two mediators of the weak force, and has an electric charge $\pm e$. It has the potential to violate several conservation laws obeyed by electromagnetic and strong interactions, such as flavor, isospin, and parity conservation. Weak decays allow for fermions to change from one flavor to another; in beta decay for instance, an up quark u can change flavor into a down quark d by emitting a virtual W boson which then decays into $e^+\nu_e$. Leptonic decay modes of the W boson have been well measured at e^+e^-, $p\bar{p}$, and pp colliders, with this being the preferred method for obtaining the W mass. However all leptonic decays of the W boson involve a neutrino which is not seen by todays detectors, thus no fully reconstructed leptonic decays have been measured. There are also no existing measurements of fully reconstructed exclusive hadronic W decays. Most measurements taken of hadronic W decays involve columnated sprays of hadrons called jets, making full reconstruction difficult due to the number of resulting daughter hadrons. Only ten branching fractions have been measured for the W boson [2], shown in Fig 2

W^+ DECAY MODES

W^- modes are charge conjugates of the modes below.

	Mode		Fraction (Γ_i/Γ)		Confidence level
Γ_1	$\ell^+\nu$	[a]	(10.80 ± 0.09) %		
Γ_2	$e^+\nu$		(10.75 ± 0.13) %		
Γ_3	$\mu^+\nu$		(10.57 ± 0.15) %		
Γ_4	$\tau^+\nu$		(11.25 ± 0.20) %		
Γ_5	hadrons		(67.60 ± 0.27) %		
Γ_6	$\pi^+\gamma$		< 8	$\times 10^{-5}$	95%
Γ_7	$D_s^+\gamma$		< 1.3	$\times 10^{-3}$	95%
Γ_8	cX		(33.4 ± 2.6) %		
Γ_9	$c\bar{s}$		(31 $^{+13}_{-11}$) %		
Γ_{10}	invisible	[b]	(1.4 ± 2.9) %		

[a] ℓ indicates each type of lepton (e, μ, and τ), not sum over them.

[b] This represents the width for the decay of the W boson into a charged particle with momentum below detectability, p< 200 MeV.

FIG. 2. Observed Decay Modes of the W Boson

C. Particle Decay Reconstruction

The reconstruction of particle decays is done using relatavistic calculations. For multiple particles coming from the same decay vertex we can apply conservation laws and deduce that the four vector of the decaying particle is equal to the sum of the four vectors of the daughter particles. Thus, one can use this sum of four vectors to calculate invariant mass, which is taken to be the mass of the decaying particle. The relation between energy, mass, and momentum is $E^2 = p^2c^2 + m_0^2c^4$.

II. EXPERIMENTAL SETUP

Data used in the search was collected at the Collider Detecor at Fermilab (CDF) during Run II. Millions of collisions per second occur within CDF during runtime, making it crucial to employ a triggering system which only accepts events yielding interesting physics phenomena to study. Data we use consists of events that passed the Silicon Vertex Trigger (SVT) system, with information about each of these events saved by the CDF data acquisition system. The CDF tracking system, Silicon Vertex Trigger, and experimental data flow will be discussed in this section.

A. Detector

CDF is a multipurpose detecor in which protons and antiprotons are collided with a center of mass energy of 1.96 TeV. The detector is pictured in Fig 3.

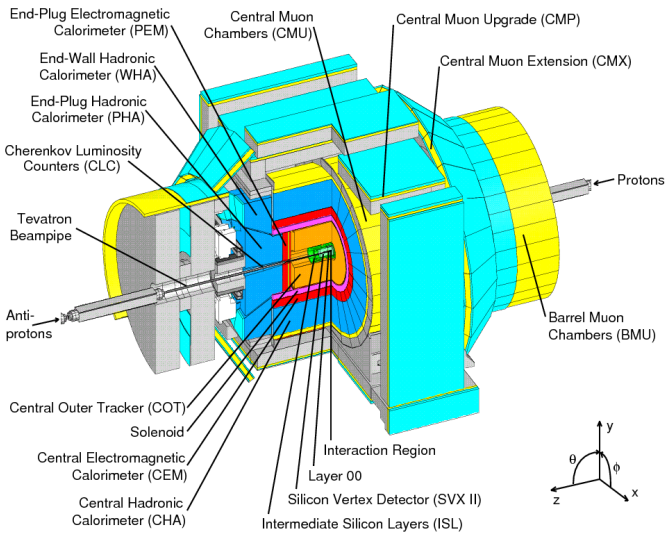

FIG. 3. CDF Detector

The CDF tracking system is placed inside a superconducting solenoid of radius 1.5 m and length 4.8 m, and a magnetic field of 1.4 T parallel to the beam axis [3]. Outside of the interaction region there are multiple layers of silicon for tracking (Layer 00, SVX II, and Intermediate Silicon Layers). A large drift chamber called the Central Outer Tracker (COT) with radial coverege from 44 to 132 cm is located just beyond the silicon layers. A spherical coordinate system is utilized for particle tracking, where the polar angle θ is measure from the proton beam axis and the azimuthal angle ϕ is measured in a transverse plane from the x-axis. Fig. 4 shows a more detailed view of the geometry of the CDF detector and tracking system.

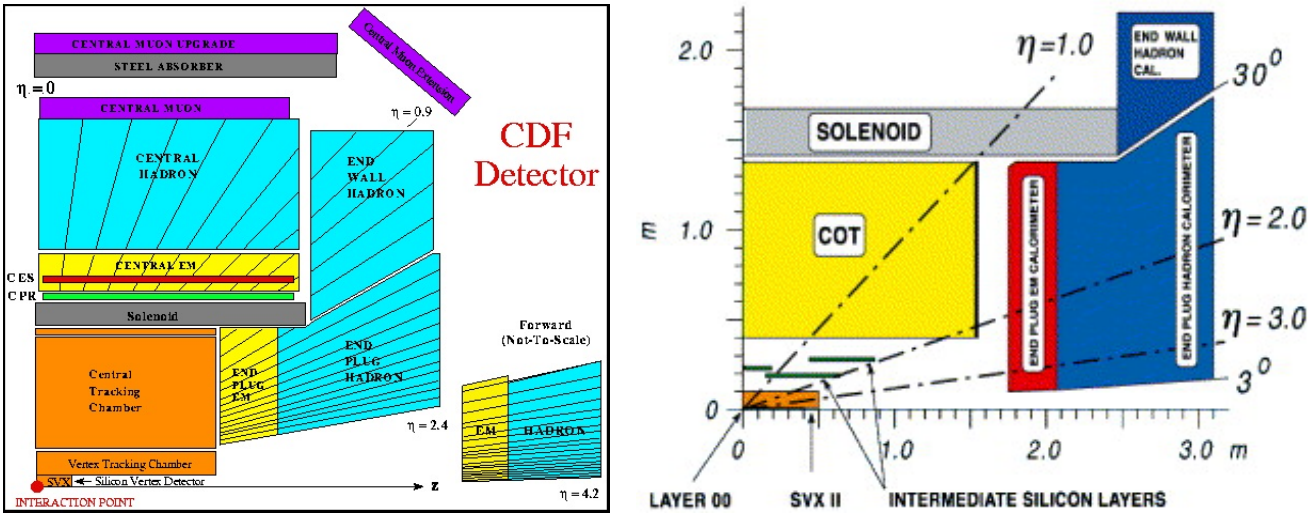

FIG. 4. CDF Detector Geometry

B. Silicon Vertex Trigger

Event selection of the Silicon Vertex Trigger is broken into three levels (L1, L2, L3); L1 and L2 are hardware based, and L3 is software based. The detector and trigger have specific geometrical acceptance; this will be discussed in terms of pseudorapidity, $\eta \equiv -\ln\left[\tan\left(\frac{\theta}{2}\right)\right]$.

1. Level 1

At L1 a device called the eXtremely Fast Tracker (XFT) [4] reconstructs tracks of charged particles in the Central Outer Tracker that lie within the central pseudorapidity region $|\ \eta\ | \leq 1$. A minimum 2 charged track requirement with angular seperation smaller than 135° is needed in

order for an event to pass L1 [4, 5], with each track having $P_T > 2\ GeV/c$. Track momentum, position, and curvature are estimated from the COT data and this information is passed to L2 if the L1 requirements are satisfied in a given event.

2. Level 2

At L2 the SVT takes a readout of hit information collected by SVX II and links the hits with charged particle tracks saved by the XFT. Typical configuration requires an XFT track to coincide with hits in four of six availible silicon layers in SVX II. Using this information the SVT computes whether an event is likely to contain a displaced secondary vertex [3]. Requirements are placed at L2 on impact parameter (closest approach of a track to the beamline) to select events in which the secondary decay vertex belongs to a bottom or charm hadron. For an event to pass L2, two good SVT tracks with $P_T > 2\ GeV/c$ are required, each with an impact parameter b within the range $0.1\ mm \leq b \leq 1.0\ mm$ [5]. Events passing L2 requirements are pushed on to L3.

3. Level 3

At L3 a farm of PCs runs a full event reconstruction, utalizing software tracking to confirm the hardware tracking performed at L1 and L2 [4, 5]. Events that pass L3 are saved to disk and later written to tape in production data sets used to study physics phenomena.

C. Computing and Software

1. Data Processing

The current computing environment for the CDF experiment is the Scientific Linux 6 operating system. Interactive and batch computing are the methods availibe for processing data. Interactive data processing is favored for smaller amounts of data, and is useful for debugging code before processing the bulk of the data. During interactive processing for offsite users, CDF computers are accessed remotely and commands can be submitted for data processing on that node. For larger data processing jobs, batch computing is the preferred method. The CDF experiment uses a grid computing system named FermiGrid where large amounts of CPUs are availible to users depending on their priority. Grid jobs can be submitted from remotely accessed CDF nodes with specifications of a data set to process and an output location. All official data from the CDF

experiment is handled by SAM (Sequential data Access via Meta-data) [6] and stored on tape. SAM mediates the access and delivery of data sets, and ensures that data files are provided in the optimal order during batch data processing.

2. Programming Languages

Reconstruction, simulation, and analysis software at CDF builds off of existing software, most of which comes from the high-energy physics community. Most software for the CDF experiment [7] is written in C++, Fortran 77, and ANSI C, although vaious programming languages such as tcl, linux shell scripting, and more are implemented as well.

D. Data Flow

Fig 5 illustrates the flow of data in the CDF experiment.

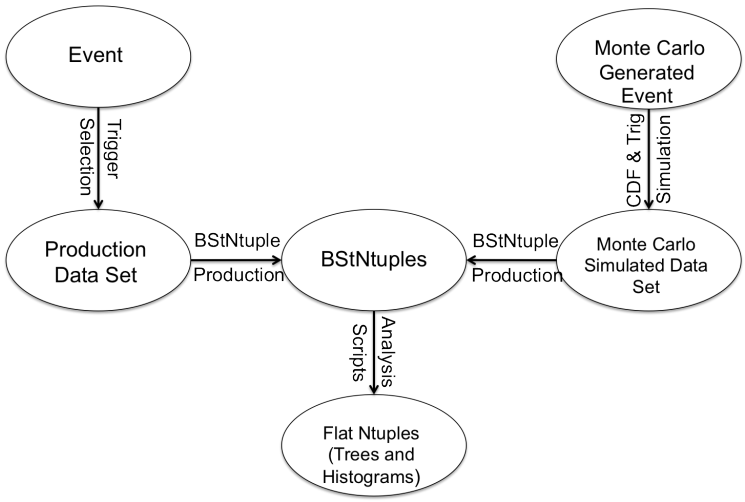

FIG. 5. CDF Data Flow

III. PROCEDURE

We search for 87 possible outcomes of exclusive $W^+ \to c\bar{s}$ decays, and the charge conjugate $W^- \to \bar{c}s$ decays that can occur during the hadronization process. Monte Carlo generated data is used in order to determine efficiencies of the trigger, reconstruction, and selection for decays in our search. The generated signal is also useful in applying cuts to reduce background and optimize our signal to background ratio in real data. We sort track information stored in production and simulated data sets into a useful format for conducting particle decay analyses called BStntuples. Detailed event selection scripts can then be implemented on data stored in BStntuples in order to determine if an event contains a decay of interest. Each exclusive decay mode of the W boson in the search is listed in Sec. III A.

A. Exclusive W Decay Modes of Interest

1. $D^+(K^-2\pi^+)K^+\pi^-$
2. $D^+(K^0_S(\pi^+\pi^-)\pi^+)K^+\pi^-$
3. $D^+(K^0_S(\pi^+\pi^-)2\pi^+\pi^-)K^+\pi^-$
4. $D^+(\phi(K^+K^-)\pi^+)K^+\pi^-$
5. $D^+(K^-2\pi^+)K^+\pi^+2\pi^-$
6. $D^+(K^0_S(\pi^+\pi^-)\pi^+)K^+\pi^+2\pi^-$
7. $D^+(K^0_S(\pi^+\pi^-)2\pi^+\pi^-)K^+\pi^+2\pi^-$
8. $D^+(\phi(K^+K^-)\pi^+)K^+\pi^+2\pi^-$
9. $D^+(K^-2\pi^+)K^0_S(\pi^+\pi^-)\pi^+\pi^-$
10. $D^+(K^0_S(\pi^+\pi^-)\pi^+)K^0_S(\pi^+\pi^-)\pi^+\pi^-$
11. $D^+(K^0_S(\pi^+\pi^-)2\pi^+\pi^-)K^0_S(\pi^+\pi^-)\pi^+\pi^-$
12. $D^+(\phi(K^+K^-)\pi^+)K^0_S(\pi^+\pi^-)\pi^+\pi^-$
13. $D^+(K^-2\pi^+)K^0_S(\pi^+\pi^-)$
14. $D^+(K^0_S(\pi^+\pi^-)\pi^+)K^0_S(\pi^+\pi^-)$
15. $D^+(K^0_S(\pi^+\pi^-)2\pi^+\pi^-)K^0_S(\pi^+\pi^-)$
16. $D^+(\phi(K^+K^-)\pi^+)K^0_S(\pi^+\pi^-)$
17. $D^0(K^-\pi^+)K^+\pi^+\pi^-$
18. $D^0(K^-2\pi^+\pi^-)K^+\pi^+\pi^-$
19. $D^0(K^0_S(\pi^+\pi^-)\pi^+\pi^-)K^+\pi^+\pi^-$
20. $D^0(K^-\pi^+)K^+$
21. $D^0(K^-2\pi^+\pi^-)K^+$
22. $D^0(K^0_S(\pi^+\pi^-)\pi^+\pi^-)K^+$
23. $D^0(K^-\pi^+)K^0_S(\pi^+\pi^-)\pi^+$
24. $D^0(K^-2\pi^+\pi^-)K^0_S(\pi^+\pi^-)\pi^+$
25. $D^0(K^0_S(\pi^+\pi^-)\pi^+\pi^-)K^0_S(\pi^+\pi^-)\pi^+$
26. $D^0(K^-\pi^+)K^0_S(\pi^+\pi^-)2\pi^+\pi^-$
27. $D^0(K^-2\pi^+\pi^-)K^0_S(\pi^+\pi^-)2\pi^+\pi^-$
28. $D^0(K^0_S(\pi^+\pi^-)\pi^+\pi^-)K^0_S(\pi^+\pi^-)2\pi^+\pi^-$
29. $D^+_s(\phi(K^+K^-)\pi^+)K^+K^-$
30. $D^+_s(\bar{K}^*(892)^0(K^+\pi^-)K^+)K^+K^-$
31. $D^+_s(K^0_S(\pi^+\pi^-)K^+)K^+K^-$
32. $D^+_s(K^0_S(\pi^+\pi^-)K^+\pi^+\pi^-)K^+K^-$
33. $D^+_s(2\pi^+\pi^-)K^+K^-$
34. $D^+_s(\phi(K^+K^-)\pi^+)K^+K^-\pi^+\pi^-$
35. $D^+_s(\bar{K}^*(892)^0(K^+\pi^-)K^+)K^+K^-\pi^+\pi^-$
36. $D^+_s(K^0_S(\pi^+\pi^-)K^+)K^+K^-\pi^+\pi^-$
37. $D^+_s(K^0_S(\pi^+\pi^-)K^+\pi^+\pi^-)K^+K^-\pi^+\pi^-$
38. $D^+_s(2\pi^+\pi^-)K^+K^-\pi^+\pi^-$
39. $D^+_s(\phi(K^+K^-)\pi^+)K^0_S(\pi^+\pi^-)\pi^+\pi^-$
40. $D^+_s(\bar{K}^*(892)^0(K^+\pi^-)K^+)K^0_S(\pi^+\pi^-)\pi^+\pi^-$
41. $D^+_s(K^0_S(\pi^+\pi^-)K^+)K^0_S(\pi^+\pi^-)\pi^+\pi^-$
42. $D^+_s(K^0_S(\pi^+\pi^-)K^+\pi^+\pi^-)K^0_S(\pi^+\pi^-)\pi^+\pi^-$
43. $D^+_s(2\pi^+\pi^-)K^0_S(\pi^+\pi^-)\pi^+\pi^-$
44. $D^*(2010)^+(D^0(K^-\pi^+)\pi^+)K^+\pi^-$
45. $D^*(2010)^+(D^0(K^-2\pi^+\pi^-)\pi^+)K^+\pi^-$
46. $D^*(2010)^+(D^0(K^0_S(\pi^+\pi^-)\pi^+\pi^-)\pi^+)K^+\pi^-$
47. $D^*(2010)^+(D^0(K^-\pi^+)\pi^+)K^+\pi^+2\pi^-$
48. $D^*(2010)^+(D^0(K^-2\pi^+\pi^-)\pi^+)K^+\pi^+2\pi^-$
49. $D^*(2010)^+(D^0(D^0(K^0_S(\pi^+\pi^-)\pi^+\pi^-)\pi^+)K^+\pi^+2\pi^-$
50. $D^*(2010)^+(D^0(K^-\pi^+)\pi^+)K^0_S(\pi^+\pi^-)\pi^+\pi^-$
51. $D^*(2010)^+(D^0(K^-2\pi^+\pi^-)\pi^+)K^0_S(\pi^+\pi^-)\pi^+\pi^-$
52. $D^*(2010)^+(D^0(K^0_S(\pi^+\pi^-)\pi^+\pi^-)\pi^+)K^0_S(\pi^+\pi^-)\pi^+\pi^-$
53. $D^*(2010)^+(D^0(K^-\pi^+)\pi^+)K^0_S(\pi^+\pi^-)$
54. $D^*(2010)^+(D^0(K^-2\pi^+\pi^-)\pi^+)K^0_S(\pi^+\pi^-)$
55. $D^*(2010)^+(D^0(K^0_S(\pi^+\pi^-)\pi^+\pi^-)\pi^+)K^0_S(\pi^+\pi^-)$
56. $D^*(2010)^+(D^0(K^-\pi^+\pi^0)\pi^+)K^+\pi^-$
57. $D^*(2010)^+(D^0(K^-2\pi^+\pi^-\pi^0)\pi^+)K^+\pi^-$
58. $D^*(2010)^+(D^0(K^0_S(\pi^+\pi^-)\pi^+\pi^-\pi^0)\pi^+)K^+\pi^-$
59. $D^*(2010)^+(D^0(K^-\pi^+)\pi^+\pi^0)K^+\pi^+2\pi^-$
60. $D^*(2010)^+(D^0(K^-2\pi^+\pi^-\pi^0)\pi^+)K^+\pi^+2\pi^-$
61. $D^*(2010)^+(D^0(D^0(K^0_S(\pi^+\pi^-)\pi^+\pi^-\pi^0)\pi^+)K^+\pi^+2\pi^-$
62. $D^*(2010)^+(D^0(K^-\pi^+)\pi^+\pi^0)K^0_S(\pi^+\pi^-)\pi^+\pi^-$
63. $D^*(2010)^+(D^0(K^-2\pi^+\pi^-\pi^0)\pi^+)K^0_S(\pi^+\pi^-)\pi^+\pi^-$
64. $D^*(2010)^+(D^0(K^0_S(\pi^+\pi^-)\pi^+\pi^-\pi^0)\pi^+)K^0_S(\pi^+\pi^-)\pi^+\pi^-$
65. $D^*(2010)^+(D^0(K^-\pi^+)\pi^+\pi^0)K^0_S(\pi^+\pi^-)$
66. $D^*(2010)^+(D^0(K^-2\pi^+\pi^-)\pi^+\pi^0)K^0_S(\pi^+\pi^-)$
67. $D^*(2010)^+(D^0(K^0_S(\pi^+\pi^-)\pi^+\pi^-)\pi^+\pi^0)K^0_S(\pi^+\pi^-)$
68. $\Lambda^+_c(pK^-\pi^+)\bar{p}K^+$
69. $\Lambda^+_c(pK^0_S(\pi^+\pi^-)\pi^+\pi^-)\bar{p}K^+$
70. $\Lambda^+_c(\Lambda^0(p\pi^-)\pi^+)\bar{p}K^+$
71. $\Lambda^+_c(\Lambda^0(p\pi^-)2\pi^+\pi^-)\bar{p}K^+$
72. $\Lambda^+_c(pK^-\pi^+)\bar{p}K^+\pi^+\pi^-$
73. $\Lambda^+_c(pK^0_S(\pi^+\pi^-)\pi^+\pi^-)\bar{p}K^+\pi^+\pi^-$
74. $\Lambda^+_c(\Lambda^0(p\pi^-)\pi^+)\bar{p}K^+\pi^+\pi^-$
75. $\Lambda^+_c(\Lambda^0(p\pi^-)2\pi^+\pi^-)\bar{p}K^+\pi^+\pi^-$
76. $\Lambda^+_c(pK^-\pi^+)\bar{p}K^0_S(\pi^+\pi^-)\pi^+$
77. $\Lambda^+_c(pK^0_S(\pi^+\pi^-)\pi^+\pi^-)\bar{p}K^0_S(\pi^+\pi^-)\pi^+$
78. $\Lambda^+_c(\Lambda^0(p\pi^-)\pi^+)\bar{p}K^0_S(\pi^+\pi^-)\pi^+$
79. $\Lambda^+_c(\Lambda^0(p\pi^-)2\pi^+\pi^-)\bar{p}K^0_S(\pi^+\pi^-)\pi^+$
80. $\Lambda^+_c(pK^-\pi^+)\Lambda^0(p\pi^-)$
81. $\Lambda^+_c(pK^0_S(\pi^+\pi^-)\pi^+\pi^-)\Lambda^0(p\pi^-)$
82. $\Lambda^+_c(\Lambda^0(p\pi^-)\pi^+)\Lambda^0(p\pi^-)$
83. $\Lambda^+_c(\Lambda^0(p\pi^-)2\pi^+\pi^-)\Lambda^0(p\pi^-)$
84. $\Lambda^+_c(pK^-\pi^+)\Lambda^0(p\pi^-)\pi^+\pi^-$
85. $\Lambda^+_c(pK^0_S(\pi^+\pi^-)\pi^+\pi^-)\Lambda^0(p\pi^-)\pi^+\pi^-$
86. $\Lambda^+_c(\Lambda^0(p\pi^-)\pi^+)\Lambda^0(p\pi^-)\pi^+\pi^-$
87. $\Lambda^+_c(\Lambda^0(p\pi^-)2\pi^+\pi^-)\Lambda^0(p\pi^-)\pi^+\pi^-$

B. Monte Carlo Production

1. Monte Carlo Integration Method

Monto Carlo integration is a method that has been proven to be very useful in high-energy physics experiments. The integration method aggregates a result using randomly generated inputs from a probability distribution over a given domain of inputs. Typical integration requires a mathematical desripction of the system, such as a partial differential equation, where the integration can become increasingly complicated as the complexity of the system increases. Monte Carlo integration assumes the system to be described by probability density functions, allowing for simpler computation of more complex systems, even when integrating over many dimensions [8]. The Monte Carlo method is implemented during event generation in order to simulate probable outcomes for reconstruction of specific decays from collisions.

2. Monte Carlo Production at CDF

Monte Carlo production at CDF [9] uses PYTHIA to generate collisions, an EvtGen package to determine how particles are allowed to decay, and GEANT to simulate the passage of particles through matter. Generated events are run through a detector simulation (cdfSim) and a trigger simulation (TRGSim++) for selection. Finally an executable (ProductionExe) performs a full event reconstruction and the output is sent to the user. We are able to generate events containing a specific decay of interest by using input files to specify an exclusive decay mode of the W boson and setting it's branching fraction to 1.0. This allows for trigger, event reconstruction, and event selection efficiency to be calculated for a given decay mode.

C. BStntuple Production

As mentioned before, a BStntuple is a compressed data format useful for reconstructing particle decays. The BStntuple production process involves a series of instruction files (tcl), an executable (CandsExe), and real or simulated data. Each decay mode of interest is written into a main tcl file in decay blocks, and assigned a reconstruction module with corresponding C++ code. A wide range of requirements may be implemented in each decay block depending on the code content of the corresponding reconstruction module. Events which pass requirements for a given decay are saved into a decay data block corresponding to a decay block in the tcl file. Information saved in

the decay data blocks can be used for further more detailed analyses. We created a tcl file including decay blocks for each W decay mode shown in Sec. III A, as well as the corresponding charm particle decays for our exclusive modes. It was necessary for us to add new reconstruction modules, and make many modifications to code for existing reconstruction modules, allowing us to use the existing methods contained within the BStntuple code; reconstruction requirements implemented during BStntuple production are outlined in Sec. III C 1. During BStntuple production it was helpful to minimize the output file size by only recording events potentially containing decays of interest. Using availibe modules we were able to accomplish this, effectively decreasing the processing time of the detailed analyses at the next level of event selection. A large portion of my summer work was spent in the BStntuple production stage, as we are examining 87 possible outcomes for exclusive decay modes of the W boson; this step required a significant amount of work.

1. BStntuple Selection Criteria

a. Transvese Momentum: Transverse momentum is the momentum of a particle measured in a plane transverse to the beam axis. A requirement on transverse momentum $P_T > 1.5\ GeV/c$ was placed on all tracks used to reconstruct W decays during the BStntuple production process. This cut discards a significant amount of tracks and is one of the first applied in the programming flow allowing for faster processing of the rest of the program. A cut of $P_T > 10.0\ GeV/c$ was placed on all charmed hadrons from 3, 4 and 5 body W decays, and a cut of $P_T > 20.0\ GeV/c$ was placed on all charmed hadrons from 2 body W decays.

b. Mass Window: Invariant mass of a particle can be calculated using the relation of mass, energy, and momentum shown in Eq. I C. The calculated invariant mass of input track collections must fall within the mass window of a decaying particle in order for an event to be selected for a given decay. We apply the requirement $m_W \geq 40$ to all W decay modes included in our analysis.

c. Decay Length: Requirements were placed on decay lengths of the W boson and charm particles for each decay as follows, $\mid l_{xyW} \mid < 250\ \mu m$ for the W boson; $l_{xyCharm} < 2.5\ cm$ for all charm particles. Requirements were also placed on the ratio of the decay length and decay length error for charm particles as follows, $\frac{l_{xyCharm}}{\sigma_{l_{xyCharm}}} > 3.0$ for all charm particles.

d. Charge Requirements: Total charge requirements were placed on combinations of charged tracks used to reconstruct decays, as well as charge product requirements to ensure that we are not reconstructing decays with incorrect charge combinations. For example, in the decay $D^{\pm} \to K^{\mp}2\pi^{\pm}$

charge requirements would ensure that only events where $\mid q_1 + q_2 + q_3 \mid = 1$, $q_1 * q_2 = -1$ and $q_2 * q_3 = 1$ are selected from track combinations.

e. Isolation: Isolation is a requirement that we placed specifically on the charm particles in our reconstructed W decays. Isolation I is defined as $I = \frac{\vec{P}_{charm}}{\sum_{i=1}^{N_{cone}} \vec{P}_i}$. Where the denominator is the sum of all charged particles within a cone of a given angle around $\vec{P}_{charm}$, the momentum vector of the charm particle. For each W decay mode in the search, cone angle for the isolation calculation was set to 0.3 radians, a fairly small cone angle to keep requirements loose at this level of event selection. A requirement on the minimum value of isolation I was then placed on each W decay mode depending on the number of daughter hadrons in the inital decay of the W boson. For 2 and 3 body decays, the requirement $I > 0.7$ was applied; for 4 body decays, the requirement $I > 0.6$ was applied; and for 5 body decays the requirement $I > 0.5$ was applied.

D. Further Analysis

The next step is to carry out further analysis of selected events, where each W decay mode in the search will have a series of corresponding analysis scripts. Information about particles within the decay are easily accessible from the produced BStntuples, therefore the analysis code needed is simplified to accesing this information, implementing tighter requirements than the previous level of event selection, and writing in new methods when needed to help ensure accurate reconstruction. This level of event selection is done within the ROOT analysis framework. ROOT is a C++ interpreter with built in classes and libraries useful for conducting research in high energy physics. We produce flat ntuples in the form of trees (TTree) and histograms (TH..) using ROOT, which can be further analyzed and fitted for results. A tree is a series of histograms organized in a useful format for analyzing decays, where information about observables of each particle in the decay are stored. The histograms show distributions of these observables, where the binning can be set suitably depending on the observable.

IV. RESULTS

A. Reonstruction, Trigger, and Selection Efficiency Calculations based on Monte Carlo Simulations

The histograms in this section show W candidate mass distributions in Monte Carlo generated signal events, with the shaded region depicting the distribution of selected candidates used for efficiency calculations. The range 76.0 $GeV/c^2 \leq m_W \leq$ 83.0 GeV/c^2 was chosen for these calculations in order to account for the full width of the W boson, $\Gamma_W = 2.085 \pm 0.042\ GeV$. The efficiency is estimated using $e = \frac{N_{Window}}{N_{Gen}}$. Where N_{Window} is the number of selected candidates within the mass window stated above, and $N_{Gen} = 22658$, the number of generated events in the Monte Carlo samples. Efficiency estimates for a few of the decay modes in the search are shown in Table I, and again beneath each of the respective mass histograms in Figs. 6-12.

TABLE I. Estimated Efficiencies of Trigger, Reconstruction, and Selection

W Boson Decay Modes	Efficiency Estimates e
$D^+(K^-2\pi^+)K^+\pi^-$	1.61%
$D^+(K^-2\pi^+)K^0_S(\pi^+\pi^-)\pi^+\pi^-$	0.45%
$D^+(K^-2\pi^+)K^+\pi^+2\pi^-$	1.32%
$D^0(K^-\pi^+)K^+\pi^+\pi^-$	0.83%
$D^+_s(\phi(K^+K^-)\pi^+)K^+K^-$	1.42%
$D^*(2010)^+(D^0(K^-\pi^+)\pi^+)K^+\pi^-$	0.78%
$\Lambda^+_c(pK^-\pi^+)\bar{p}K^+$	0.27%

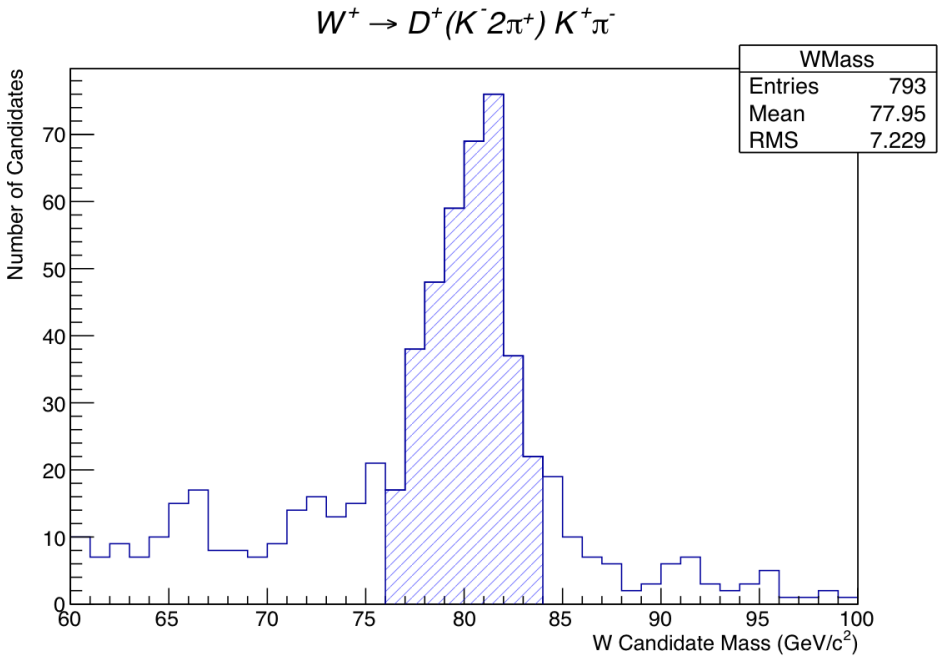

FIG. 6. Monte Carlo Simulation ($e = 1.61\%$)

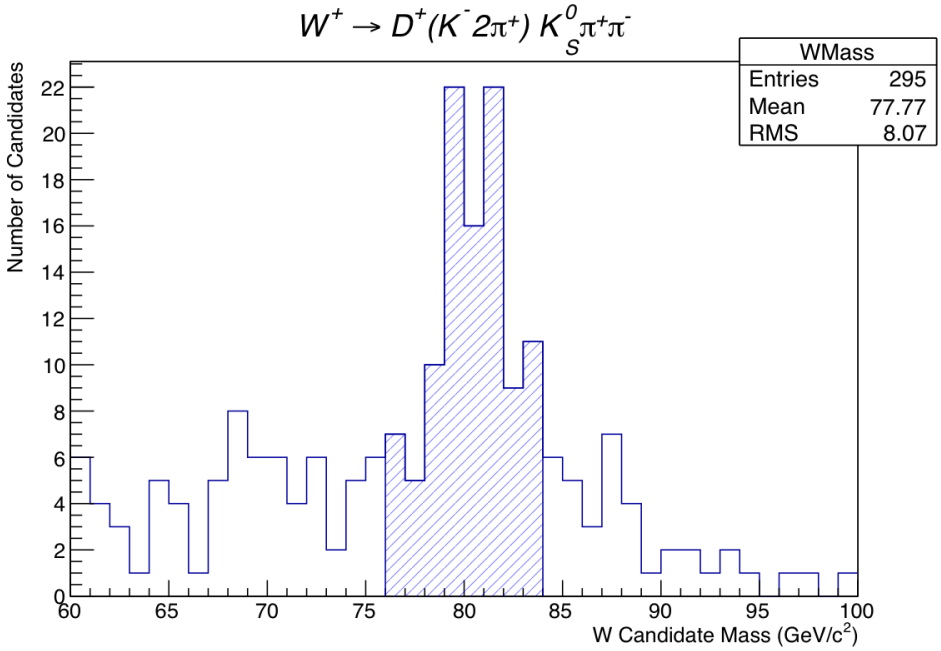

FIG. 7. Monte Carlo Simulation ($e = 0.45\%$)

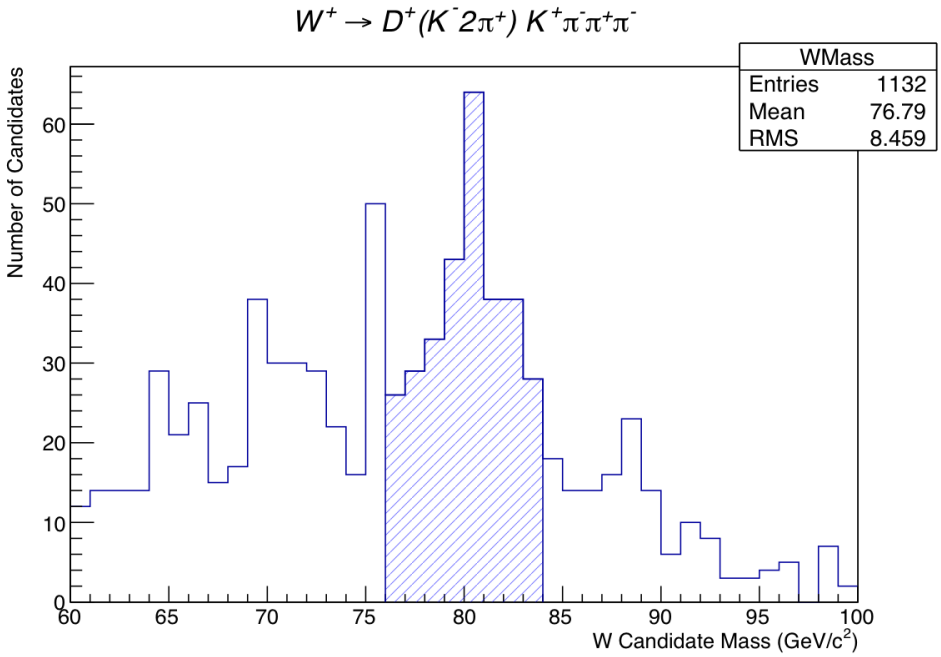

FIG. 8. Monte Carlo Simulation ($e = 1.32\%$)

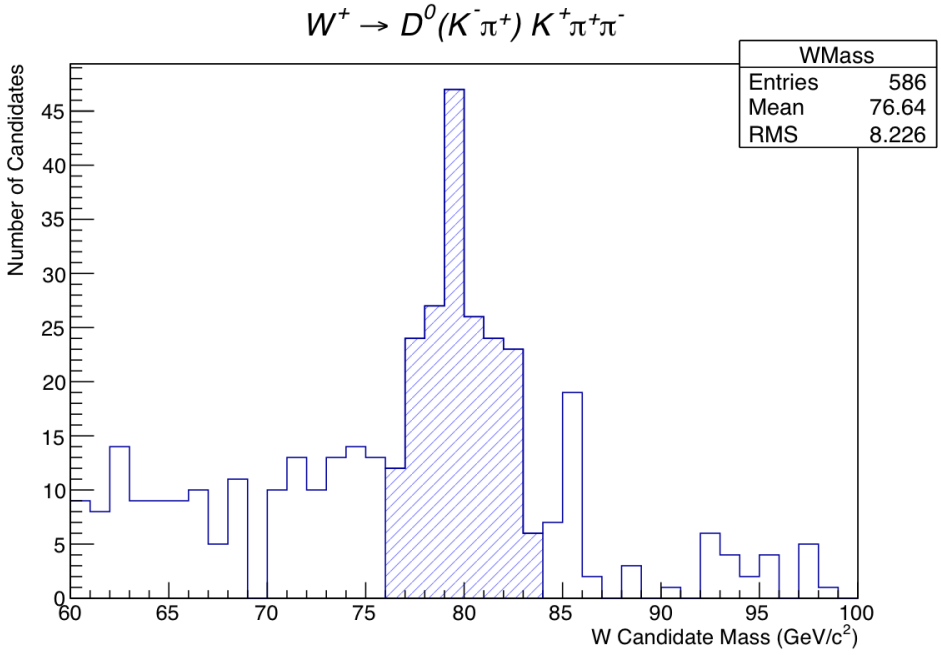

FIG. 9. Monte Carlo Simulation ($e = 0.83\%$)

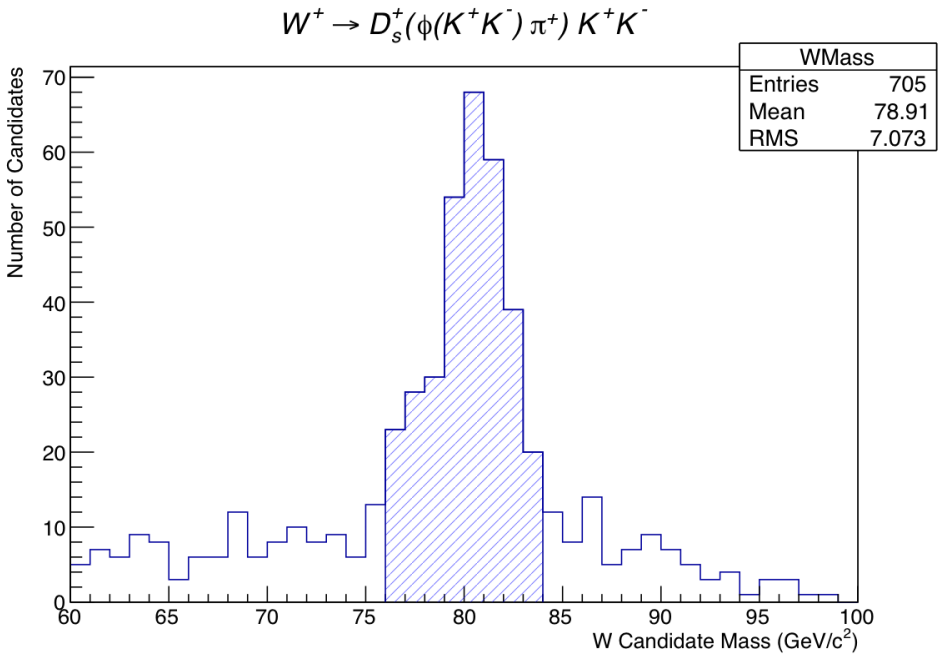

FIG. 10. Monte Carlo Simulation ($e = 1.42\%$)

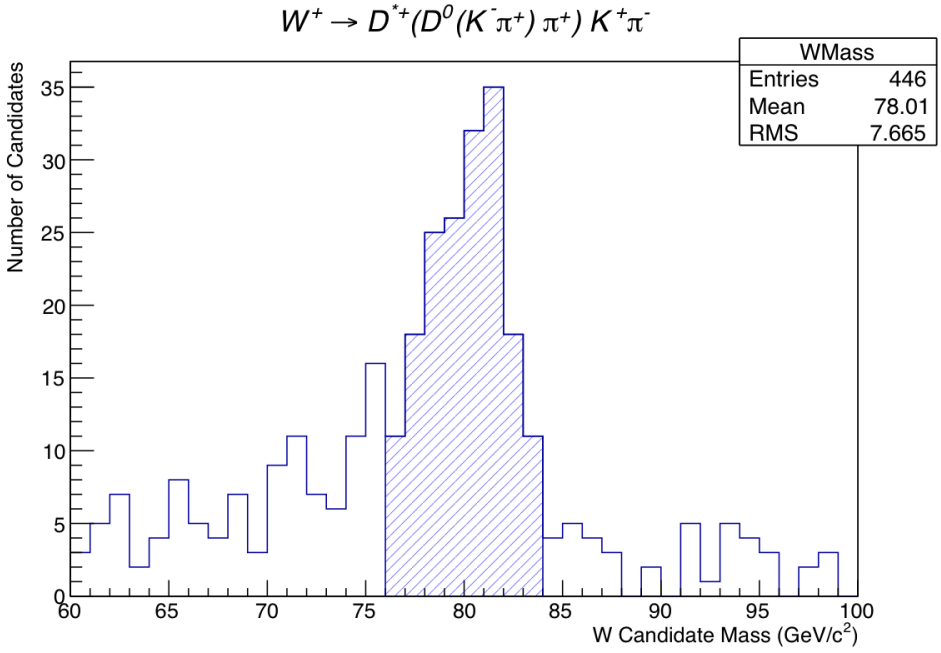

FIG. 11. Monte Carlo Simulation ($e = 0.78\%$)

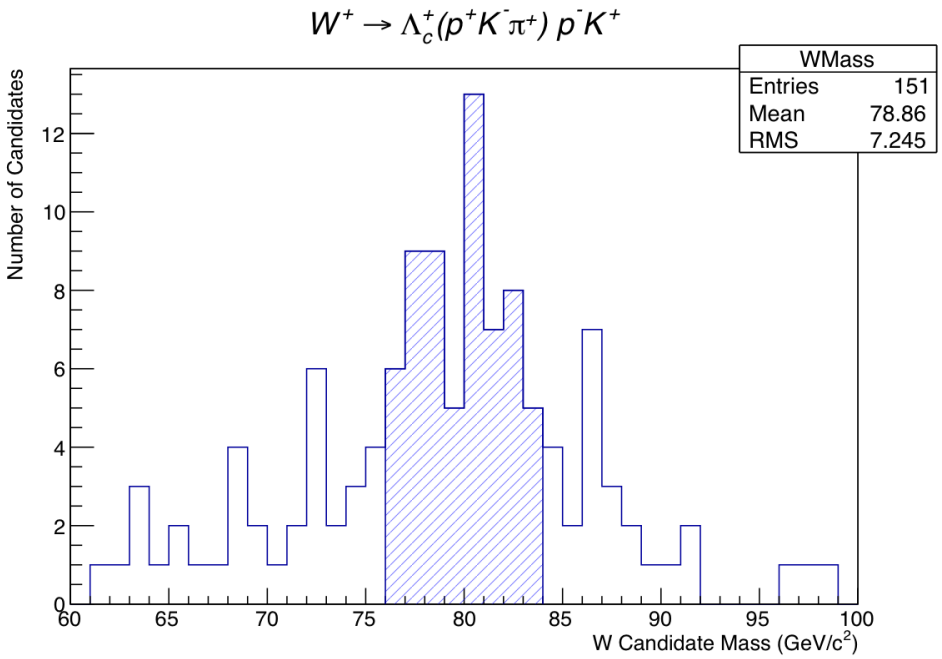

FIG. 12. Monte Carlo Simulation ($e = 0.27\%$)

V. CONCLUSION

A significant amount of work still needs to be done to determine results of the search. We are currently running BStntuple production code on roughly 350 Tb of data in order to push the analysis on to the next level of event selection. We see based on efficiency estimates shown in Sec. IV that even if one of these rare decays occurs in data, there is a limit on how well we properly reconstruct the signal. It should be noted that efficiencies will be calculated for the remaining decay modes, and experimental and systematic uncertanties will be taken into account for these calculations as well as for any findings in real data. Events of interest in the search are indeed very rare, but a full reconstruction of a W decay could potentially spark the interest of many within the high energy physics community and lead to exciting new measurements.

ACKNOWLEDGMENTS

I have truly learned a great deal during my REU experience. I would like to thank the faculty and staff of the WSU physics department for making this program possible, in particlular, my advisor Professor Robert Harr for his dedication to his students and his outstanding advising. I would also like to thank the National Science Foundation; this work was funded under NSF Grant

PHY-1460853.

---

[1] K. Grogg, (2011). *Jets Produced in Association with W-Bosons in CMS at the LHC* (Doctoral dissertation). Retrieved from http://cds.cern.ch/record/1376067/files/CERN-THESIS-2011-064.pdf

[2] K.A. Olive *et al.* (Particle Data Group), Chin. Phys. C, 38, 090001 (2014).

[3] S. Baskaran, (2015). *Search for Fully Reconstructed W Boson Decay* (Master's thesis). Retrieved from http://search.proquest.com/docview/1691327396

[4] J. Adelman, *et al.*, (2006). (CDF Collaboration), Retrieved from http://www-cdf.fnal.gov/internal/upgrades/daq_trig/trigger/svt/Papers/vtx05.pdf

[5] J. Adelman, *et al.*, (CDF Collaboration), Nucl. Instr. and Meth. A 572 (2007) 361.

[6] I. Sfiligoi, (2006). *CDF Computing* [PDF document]. Retrieved from http://www-cdf.fnal.gov/physics/talks_transp/2006/ccp2006_sfiligoi.pdf

[7] S. Lammel, (2010). *CDF Computing Infrastructure, Code Management.* Retrieved from http://www-cdf.fnal.gov/internal/fastnavigator/fastnavigator.html

[8] C. Bozzi, (2002). *Monte Carlo Simulation in Particle Physics* [PowerPoint slides]. Retrieved from www.fe.infn.it/~bozzi/iub.ppt

[9] O. Tadevosyan, (2009). *Monte Carlo Production Overview.* Retrieved from http://www-cdf.fnal.gov/internal/mcProduction/pages/Overview.html